RSC Advances

ROYAL SOCIETY OF CHEMISTRY

www.rsc.org/advances

Multiple Drugs-loaded Electrospun PLGA/gelatin Composite Nanofibers Encapsulated with Mesoporous ZnO Nanospheres for Potential Postsurgical Cancer Treatment

Jun Hu[1], Ming Li[2], Junchao Wei[1], Yong Chen[2], Yiwang Chen[*1]

[1]Department of Chemistry/Institute of Polymers, Nanchang University, 999 Xuefu Avenue, Nanchang 330031, China; [2]Institute for Advanced Study, Nanchang University, 999 Xuefu Avenue, Nanchang 330031, China

Abstract:

Multiple drugs-loaded electrospun composite nanofibrous scaffolds have attracted much interest as drug delivery vehicles for the treatment of tissue defect after tumor resection. In this study, a novel mesoporous ZnO/poly(lactic-co-glycolic acid)/gelatin (mZnO/PLGA/GE) electrospun composite fiber encapsulated with both hydrophilic drug (doxorubicin hydrochloride, DOX) and hydrophobic drug (camptothecin, CPT) is fabricated. mZnO is firstly used to encapsulate DOX. Then, the DOX-loaded mZnO (DOX@mZnO) and CPT were mixed with PLGA/GE solution to fabricate electrospun hybrid nanofibers. The *in vitro* release results demonstrated that the CPT in the composite fibers presented a fast release manner, while DOX showed a sustained release behavior. The cell cytotoxicity test indicated that the composite nanofiber with two drugs showed strong antitumor efficacy against HepG-2 cells. Moreover, the addition of GE increased the hydrophilicity of composite fibers. More importantly, the incorporated of mZnO within PLGA/GE nanofibers can not only significantly reduce the burst release of DOX, but also improve the mechanical durability of the composite nanofibers. Thus, the composite nanofibers could be a versatile drug delivery system encapsulated with both hydrophilic and hydrophobic anticancer drugs as implantable scaffolds for potential postsurgical cancer treatment.

Keywords: Electrospin; Nanofibers; Mesoporous ZnO; Drug delivery

[*] Corresponding author. Tel.: +86 791 83969562; fax: +86 791 83969561. *E-mail address*: ywchen@ncu.edu.cn (Y. Chen).

Introduction

In clinical treatment, patients suffer from local tumor recurrence which is usually caused by inadequate resection or implantation during surgery.[1] Taking antitumor drugs orally or by systematic injection are commonly used for adjuvant therapies after surgical resection to reduce the risk of local recurrence, but these therapies frequently showed severe side effects resulted from the spread of drugs to the healthy site.[2] Additionally, the immediate repair and reconstruction of tissue defects are of great importance for long-term successful healing in many cancer therapies after tumor resection.[3] Thus, it is desirable to develop an implantable local drug delivery scaffold. Locally controlled release systems demonstrated great potential in delivering anticancer drugs compared to conventional dosage forms, such as improved therapeutic effect, reduced toxicity, convenience, good stability and locally controlling drug release.[4] The electrospun fibers have showed various advantages such as simplicity of fabrication method, diversity of materials suitable for processing into fibers, high surface area and a complex porous structure, which have been widely used in tissue engineering scaffolds and drug delivery as locally controlled release systems.[5] The nanofibrous scaffolds can delivere anticancer drugs to kill tumor cells and provide a favorable microenvironment for tissue construction, contributing a long-term tumor healing.[1]

Presently, most electrospun fibers for drug delivery have focused on the sustained release of a single drug,[6, 7] which often can not satisfy the requirements in clinical therapies.[8] It is generally accepted that a single carrier for multi-drugs are useful to overcome drug resistance and maximized antitumor activity by harnessing different anticancer drugs with distinct characteristics and action mechanisms.[9, 10] Particularly, the multi-drugs delivery system loaded with hydrophobic and hydrophilic drugs simultaneously have great potential application for wound healing after tumor resection.[9] However, there are some challenges to realize multiple drugs safely loaded within the fiber matrix and make different drugs release independently at proper time,[11] furthermore control the burst release of hydrophilic drugs such as DOX.[12] Recently, most core-shell fibers have been prepared by coaxial[13, 14] and emulsion

electrospinning [15-17], which may load two drugs and weaken the initial burst release to achieve drugs sustained release profiles. However, the coaxial electrospinning might need substantial optimization of the electrospinning conditions, and the emulsifier used in emulsion electrospinning was difficult to remove and might introduce biocompatibility issues.[18] In order to overcome these limitations, novel drug delivery systems were fabricated by incorporating nanoscale carriers such as halloysite nanotube,[18] hydroxyapatite,[19] mesoporous nanoparticles[9, 20, 21] and polymeric nanoparticles[22, 23] into electrospun fibers. Chang et al.[20]designed dual drug-loaded poly(lactic-co-glycolic acid)/mesoporous silica nanoparticles electrospinning composite materials loaded two model fluorescent dyes, which can release in distinct release kinetics. Shi et al.[18, 19] reported an electrospun poly(lactic-co-glycolic acid)/hydroxyapatite and poly(lactic-co-glycolic acid)/halloysite nanotube composite nanofibers-based drug delivery system for DOX and tetracycline hydrochloride encapsulation and sustained release. Although previous researches[9, 18-23] have reported that nanoscale carriers embedded electrospun fiber mats could deliver one hydrophilic drug or two model fluorescent dyes in well-controlled release kinetics, the development of such a drug delivery system loaded with hydrophobic and hydrophilic anti-cancer drugs for postsurgical cancer treatment had been rarely reported.

PLGA is a FDA-approved biodegradable polymer which has been electrospun into nanofibers and widely been explored in the biomedical field for many years due to its excellent biocompatibility, controllable degradation and suitable mechanical property.[24, 25] However, PLGA fails to provide a desired microenvironment for cell adhesion due to lack of surface cell discrimination points and its intrinsic hydrophobicity.[26] Gelatin is a widely-used, water-soluble natural biopolymer derived from collagen with the advantage of low antigenicity and high biocompatibility and bioabsorptivity,[27] which can be blended with PLGA fibers to obtain a scaffold with desired biocompatible properties with cell adhesion and proliferation.[28] Nevertheless, the application of PLGA/GE nanofibers as a drug carrier is quite limited due to its drawbacks of weak mechanical durability and burst release of the drug via simply electrospinning the mixture of drug and PLGA/GE nanofibers. Recently, mZnO has

received considerable attention as candidate matrices for drug delivery carriers with the advantage of good biocompatibility, antibacterial property and high capacity of loading drug.[29-32] However, to the best of our knowledge, no reports have been published about such electrospun polymer/mZnO composite nanofibers for drug delivery.

In the present work, novel co-delivery carrier mZnO/PLGA/GE electrospun composite nanofibers encapsulated with both hydrophilic drug (DOX) and hydrophobic drug (CPT) were fabricated. mZnO was firstly used as carriers for DOX, then the DOX@mZnO and CPT were embedded in PLGA/GE nanofibers using electrospinning. The physicochemical properties, drug entrapment, and *in vitro* drug release of composite nanofiber were investigated. The results showed that incorporated of mZnO within PLGA/GE nanofibers can not only significantly reduce the burst release of the hydrophilic drug, but also improve the mechanical durability of the PLGA/GE nanofibers. In addition, the *in vitro* cell test demonstrated the composite nanofibers showed strong antitumor efficacy against HepG-2 cells.

Experimental section

Materials

Poly(lactide-co-glycolide)(PLGA, weight-average molecular weight, Mw=10kDa with LA/GA=50:50) was purchased from Daigang company (Jinan, China). Doxorubicin hydrochloride (DOX) and camptothecin (CPT) was purchased from Aldrich and used as received. Gelatin (GE, type A from porcine skin, 300 bloom), zinc acetate dihydrate ($Zn(OAc)_2 \cdot 2H_2O$, 99%), diethylene glycol (DEG, AR) and 1,1,1,3,3,3-Hexafluoro-2-propanol (HFP, AR) were purchased from Tianjin Damao Chemical Reagent Factory. Dulbecco's Modified Eagle's Medium (DMEM, KGM1640) and Newborn Calf serum were purchased from KenGEN Biotech Company. 3-(4,5-dimethylthiazolyl-2)-2,5-diphenyl tetrazolium bromide (MTT) was obtained from Aladdin reagent. Human liver carcinoma HepG2 cell was purchased from Shanghai cell center (Chinese Academy of Sciences). Other reagents were commercially available and used as received.

Preparation of DOX@mZnO

mZnO nanoparticles were synthesized according to reported literature.[29, 33] Briefly, 15 mmol of $Zn(OAc)_2$ in 150 mL of DEG was heated to 160-165 °C under reflux for 0.5 h. The resulting precipitates were separated by centrifugation, washed with deionized water and ethanol, and afterwards vacuum drying at 60 °C.

The anticancer agent DOX was used as a model drug to load into mZnO. Briefly, 200 mg mZnO was first dispersed in water (20 mL) with sonication for 1 h before use. Subsequently, 25 mg DOX was dissolved into the above mZnO aqueous dispersion under mild stirring (50 rpm) and the mixture was stirred in dark conditions at room temperature for 24 h. Then the DOX@mZnO nanohybrid was separated by centrifugation with 12000 rpm at 4 °C for 10 min and washed three times with water to remove the excess free DOX. The supernatant was analyze using a Lambda 750 UV-vis spectrophotometer (Perkin Elmer, USA) at 481 nm with a standard absorbance/concentration calibration curve at the same wavelength.[34] Finally, the DOX@mZnO particles were obtained by lyophilization and stored at 4 °C . The drug loading percentage was calculated as follows:

$$\text{Loading efficiency} = M_{DOX}/(M_{DOX}+M_{mZnO})\times 100\%$$

where M_{DOX} and M_{mZnO} were the mass of the encapsulated DOX and mZnO, respectively.

Preparation of drug-loaded composite nanofibers

The fabrication procedure of the electrospun PLGA/GE composite nanofibers encapsulated with mZnO was shown in **Fig. 1**. PLGA/GE (m/m=3:1) with an optimized concentration (16 %, w/v) was dissolved in a solvent of HFP. After that, DOX@mZnO (1 wt% DOX relative to composite nanofibers) and CPT (1 wt% relative to composite nanofibers) were blended with the PLGA/GE solution for subsequent electrospinning. As controls, a measured weight of mZnO (the same mZnO weight ratio relative to the composite nanofibers), DOX (1 wt% relative to composite nanofibers) and DOX@mZnO (1 wt% DOX relative to composite nanofibers) were separately added into PLGA/GE solution with continuous stirring to

obtain homogeneous solutions. PLGA, PLGA/GE, mZnO/PLGA/GE, DOX/PLGA/GE, DOX@mZnO/PLGA/GE and CPT/DOX@mZnO/PLGA/GE nanofibers were fabricated via electrospinning. The electrospinning process was carried out under ambient conditions with a fixed electrical potential of 18-20 kV, a tip-to-collector distance of 15 cm, and a feeding rate of 20 μL min^{-1} by the syringe pump through a blunted stainless steel needle (ID = 22 μm). After electrospinning, the nanofibers were collected on the expansion cylinder rotating at 200 rpm and vacuum dried for at least 48 h to remove residual organic solvent and moisture.

-----Fig. 1-----

Characterization

The morphologies of mZnO and electrospun fibers were characterized by scanning electron microscopy (SEM, FEI Quanta 200SEM) and field emission transmission electron microscopy (FETEM; JEOL, JEM-2100F), respectively. The particle size distribution of mZnO was determined using a Britain Malvern PSA (NANO2590) submicron particle size analyzer with angle detection at 90°. The average diameter of nanofibers was obtained from at least 100 measurements on a typical SEM image (×10000 magnification) using Nano Measurer 1.2 software. Nitrogen sorption isotherms were measured with an accelerated surface area and porosimetry system (Micromeritics ASAP2020, USA). The water contact angles of the electrospun nanofibers were estimated by the water contact angels instrument (JC2000A). The crystalline states of mZnO and fiber mats were analyzed by a Bruker D8 Focus X-ray diffractometer, a voltage of 30 kV and a current of 20 mA using a CuK_{α} radiation (λ = 0.154 nm), and continuous scan mode at the speed of 1 °/min in the range of 5-60° (2θ). The tensile testing of the composite nanofibers was performed using a SANS WDW universal test system (CMT8502) with electronic data evaluation using a 50 N load cell under a crosshead speed of 10 mm/min. All samples were prepared in rectangular shape with dimensions of 50 mm×10 mm ×80-90 μm (L ×W× T). At least five samples were tested for each type of electrospun fiber.

***In vitro* drug release**

The release kinetics of DOX and CPT were using an UV-vis spectrophotometer (Hitachi UV-3010) at an optical wavelength of 481 nm and 370 nm. The electrospun nanofiber samples were cut into pieces of 30 mg mass and placed into different vials containing 20 mL phosphate buffered saline (PBS, pH 7.4). All the vials were incubated in a horizontal laboratory shaker with a shaking speed of 400 rpm at 37 °C. At selected time intervals, 1 mL of solution was removed from each vial and analyzed using UV-vis spectroscopy and replaced with an equal volume of fresh buffer solution. Experiments were run in triplicate per sample.

Cell culture and MTT assay

HepG-2 cells were cultured in DMEM medium supplemented with 10% FBS, 100 U/mL penicillin and 100 μg/mL streptomycin. The cells were cultured at 37 °C in a humidified atmosphere containing 5% CO_2, and the medium was replaced every 2 days. For all experiments, cells were harvested by using trypsin solution and resuspended in fresh DMEM medium. Prior to cell seeding, the electrospun nanofibers were sterilized under UV light for 3 h and washed with PBS for three times.

The cytotoxicity of DOX@mZnO/PLGA/GE and CPT/DOX@mZnO/PLGA/GE composite nanofibers against HepG-2 cells was evaluated by the MTT assay after treatment of cells with electrospun nanofibers, and the cytotoxicity of mZnO/PLGA/GE and DOX/PLGA/GE nanofibers with the equivalent of fibers were also tested for comparison. Briefly, HepG-2 cells (8×10^3 cells/well) were seeded in 96-well plates and incubated overnight at 37 °C to allow cells to attach, then the medium was replaced with fresh medium and the medium containing mZnO/PLGA/GE, DOX/PLGA/GE, DOX@mZnO/PLGA/GE and CPT/DOX@mZnO/PLGA/GE composite nanofibers at the total DOX concentration of 25 μg/mL. After incubation for another 24 h and 48 h, 20 μL of MTT solution (5 mg/mL) was added to each well and followed by incubation for another 4 h. After that, the solution in the wells was deserted completely and 200 μL DMSO was added to each well to dissolve the precipitate for 15 min. And subsequently the absorbance at

578 nm was detected using an ELISA microplate reader. The relative cell viability was calculated by $[OD]_{test}/[OD]_{control} \times 100\%$, and the average value and standard deviation from the triplicate parallel sample for each fiber were reported.

Cell morphology observation

The morphologies of HepG-2 cells treated with composite nanofibers were analyzed using confocal laser scanning microscopy (CLSM: ZEISS LSM 710, Germany). Briefly, HepG-2 cells (8×10^4 cells/well) were seeded in 6-well plates and incubated overnight at 37 °C to allow cells to attach, then the medium was replaced with fresh medium and the medium containing mZnO/PLGA/GE, DOX/PLGA/GE, DOX@mZnO/PLGA/GE and CPT/DOX@mZnO/PLGA/GE composite nanofibers at the total DOX concentration of 25 μg/mL. After incubation for another 24 h and 48 h, the cell morphology was observed using CLSM.

Statistical analysis

All the data in this paper were conducted at least three times and presented as mean±standard deviation and were analyzed using Student's t-test for calculation of significance level of the data. The criteria for statistical significance were $p \leq 0.05$.

Results and Discussion

Morphology and structure of mZnO

As seen from **Fig. 2A-E**, mZnOs were fairly well-defined and discrete spherical shaped assemblies comprising of numerous fine nanocrystals from the SEM micrographs (**Fig. 2A**), and the average hydrodynamic diameter was 284.7 nm with a polydispersity index of 0.43 measured by DLS (**Fig. 2C**). **Fig. 2B** showed a TEM micrograph of a single ZnO nanoassembly, it could be seen that these spherical assemblies were highly porous in nature, which was made up of 3D spatially connected numerous nanocrystals. The pore shapes were irregular and the pore sizes were not uniform. Some previous researches[29, 35] had discussed the formation of these spherically-shaped porous assemblies by oriented attachment of nanocrystals during

the course of the synthesis. The nitrogen adsorption-desorption isotherms and pore size distribution data of mZnO were showed in **Fig. 2D** and **Fig. 2E**, which illustrated a typical type IV curve accompanied by a H3 hysteresis loop. The BET surface area was calculated to be 84.78 m^2g^{-1} and the pore size distribution was quite broad as determined via BJH method (6.75 nm). These results indicated these porous assemblies possessed great potential application as a novel drug carrier.

-----Fig. 2-----

Characterization of composite nanofibers

The morphology and diameter distribution of the PLGA/GE, DOX/PLGA/GE and DOX@mZnO/PLGA/GE electrospun fibers were shown in **Fig. 3**. The mean fiber diameters were 430 nm, 400 nm and 370 nm corresponding to the PLGA/GE, DOX/PLGA/GE and DOX@mZnO/PLGA/GE electrospun fibers with broader distribution, respectively. It might be that the addition of GE increased charge density of the jet during the electrospinning process, which resulted in decreasing of composite solution viscosity and the improvement of stretching force and the self-repulsion.[26] The surface of the PLGA/GE, DOX/PLGA/GE electrospun fibers were smooth, and no presence of DOX@mZnO nanoparticles was observed on the surface of fibers. However, the composite DOX@mZnO/PLGA/GE nanofibers appeared to become rough, with a few of protrusions being clearly seen on the surface of the fibers after adding DOX@mZnO nanoparticles. The structure of DOX@mZnO/PLGA/GE nanofibers were showed in **Fig. 4**, it indicated that the DOX@mZnO spheres were well distributed within the composite fibers and some spheres were located near the surface of the fibers forming the protrusions, which was consistent with the SEM images. In addition, as shown in **Fig. 3D-F**, the average diameter of the nanofibers decreased after incorporation of DOX and DOX@mZnO, respectively, which might be due to change of the electrospinning solution properties (such as conductivity or viscosity).[19]

-----Fig. 3-----

-----Fig. 4-----

Surface wettability was important for optimal application of electrospun fibers as drug carriers, tissue growth scaffolds, and wound-dressing materials. **Fig. 5A** showed the varied water contact angles on the surface of nanofibrous mats at about 30s, and the water contact angles after 1s, 30s and 60s were summarized in **Table 1**, respectively. It could be seen that the water contact angles of the PLGA/GE fibers decreased from 115±0.8^{o} to 55±7.8^{o} after 30s and that of the PLGA fibers were higher than 120^{o} and almost did not change after 30 s, which indicated GE enhanced the hydrophilicity of PLGA/GE nanofibers. In addition, the hydrophilicity of DOX/PLGA/GE, DOX@mZnO/PLGA/GE and CPT/DOX@mZnO/PLGA/GE fibers were better than that of PLGA/GE fibers, because the hydrophilic drug DOX might move onto the fibers surface by forces of electric and located on the fiber surface.

The XRD patterns of mZnO, PLGA/GE, DOX@mZnO/PLGA/GE and CPT/DOX@mZnO/PLGA/GE composite nanofibers were shown in **Fig. 5B**. The peaks at 2θ= 31.73°, 34.31°, 36.02°, 47.58° and 56.42° indexing (100), (002), (101), (102) and (110) were observed in the XRD pattern of mZnO, which was consistent with the results of previous studies.[29, 32] Furthermore, the PLGA/GE nanofibers only displayed a broad diffraction peak at 2θ value of 16.8°, which revealed that PLGA/GE nanofibers were amorphous. The XRD curves of the DOX@mZnO/PLGA/GE and CPT/DOX@mZnO/PLGA/GE composite nanofibers were similar to the PLGA/GE fiber curve and most peaks of the mZnO were not observed. The absence of mZnO peaks indicated that most of mZnO were well dispersed within the composite fibers.[36]

Mechanical strength should be considered in practical applications such as tissue engineering scaffold and implants. The typical tensile strain-stress curves of PLGA, PLGA/GE, DOX/PLGA/GE and DOX@mZnO/PLGA/GE composite nanofibers were shown in **Fig. S1**, and the averages of the mechanical properties were summarized in **Table 2**. The modulus or elongation of PLGA/GE fibers were 47.3±12.1 MPa or 50.5±0.7%, respectively, which sharply decreased compared to that of PLGA fibers. The addition of the gelatin decreased the mechanical properties of PLGA/gelatin

compositen fibers, which was similar to the relevant report.[26] When DOX was encapsulated, the tensile strength (2.7±0.1 MPa) and modulus (79.7±3.7 MPa) of the DOX/PLGA/GE fibers improved, while the elongation of that had a little decreased. It was due to the strong interactions between DOX and PLGA/GE, and DOX in the fibers restricting the movement of the polymer chains during stretching.[37, 38] Furthermore, it was clear that tensile strength and modulus of the DOX@mZnO/PLGA/GE nanofibers were 3.1±0.5 MPa and 136.5±5.3 MPa, which were significantly improved when compared with the PLGA/GE fibers. And this could be ascribed to not only the hard inorganic component mZnO,[19, 39] but also the frictional forces between fibers and interlocking of fiber under effect of strain, which proved by the mZnO inclusion on the subsurface of DOX@mZnO/PLGA/GE as reflecting in TEM micrographs,[40, 41] and thereby they provide frictional interlocking and better tensile strength. The slightly decreased failure strain of DOX@mZnO/PLGA/GE might be due to the increased brittleness of the fibers after doping with hard inorganic particles mZnO.[19]

-----Table 1-----

-----Table 2-----

-----Fig. 5-----

Drugs loading and release profiles

The loading content of DOX into mZnO was found to be about 9.09%, and some DOX molecules might form some complexes with ZnO during the loading process due to the interaction of DOX with ZnO, which was explored via fluorescence spectroscopy and revealed by change in the colour of the DOX solution **(Fig. S2)**. The fluorescence intensity of DOX was correspondingly plummeted and the color of the solution changed from red to purple after adding the mZnO. This phenomenon was reported and discussed in some previous works.[29, 32]

The drug release profiles of DOX and CPT from different composite electrospun fibers were evaluated. The release profiles of DOX from DOX/PLGA/GE, DOX@mZnO/PLGA/GE and CPT/DOX@mZnO/PLGA/GE fibers were shown in

Fig. 6A. As could be seen, the release of DOX from DOX/PLGA/GE fibers was significantly faster than that from both DOX@mZnO/PLGA/GE and CPT/DOX@mZnO/PLGA/GE fibers, about 41.3% of the drug was released within 20 h, and reached to a plateau after 120 h. The DOX released from the PLGA/GE scaffold showed two release stages: a burst release stage and followed gradually increased stage, and the burst release stage was mainly dependent on the water transport in the GE phase, therefore hydrophilic drug DOX molecule had a more rapid diffusion from the matrix into the aqueous medium.[42, 43] While both DOX@mZnO/PLGA/GE and CPT/DOX@mZnO/PLGA/GE fibers had a similar release manner and displayed a sustained release profile, with only 13.3% and 16.7% of DOX within 20 h, and the total amount of DOX released was 40% and 42.6 % after 120 h, respectively. The reason of sustained release should be that the DOX need to be first released from mZnO to the PLGA/GE matrix, and then from the PLGA/GE matrix to the releasing medium, thus avoiding the burst release effect signigicantly.[19] Next, the CPT and DOX releasing behaviors of CPT/DOX@mZnO/PLGA/GE fibers were measured. As seen from **Fig. 6B**, the CPT showed a burst release manner during the first 20 h, with the 30.7% within 20 h and 61.3% after 120h. The fast release of CPT was also attributed to the random distribution of CPT in the fiber matrixes and the hydrophilic phase GE, although the CPT was hydrophobic drug. Likewise, DOX was released in a similar manner from the CPT/DOX@mZnO/PLGA/GE, and showed a more sustained and longer-term release profile than did CPT. Therefore, the CPT/DOX@mZnO/PLGA/GE could be formulated as a drug-containing scaffolding material for both tissue engineering and sustained drug delivery.

-----Fig. 6-----

***In vitro* cytotoxicity effect on HepG-2 cells**

To verify the pharmacological activity of the released drugs, the cytotoxicity of the composite nanofibers against the HepG-2 cells were evaluated by MTT assay after treated with different samples for 24 h and 48 h. As shown in **Fig. 7**, no apparent

toxicity was observed for mZnO/PLGA/GE, and the cell viability was still as high as 90%. The cytotoxicity of DOX/PLGA/GE, DOX@mZnO/PLGA/GE and CPT/DOX@mZnO/PLGA/GE composite nanofibers against HepG-2 cells were increased as the increase of incubation time. However, the DOX@mZnO/PLGA/GE composite nanofibers showed statistically significant lower inhibition effect than DOX/PLGA/GE from 24 h to 48 h, which was due to the slow release rate of DOX from the composite DOX@mZnO/PLGA/GE and the a lower DOX concentration in the medium. Moreover, the cytotoxicity of CPT/DOX@mZnO/PLGA/GE composite nanofibers was similar to DOX/PLGA/GE nanofibers, which was statistically significant higher than that of DOX@mZnO/PLGA/GE composite nanofibers, and the cell viability decreased from 57.51±2.14% to 35.02± 0.42% from 24 h to 48 h. This was probably because that CPT had a rapider release in the dual drugs delivery system and the cytotoxicity might be maximized when two anticancer drugs with distinct characteristics and action mechanisms were delivered simultaneously to the cancer cells and synergistically to kill the cancer cells.

-----Fig. 7----

Cells morphology

To further confirm the antitumor activity of the medicated composite nanofibers, the morphological changes of HepG-2 cells treated with different nanofibers for 24 h and 48 h were observed by CLSM. **Fig. S3** showed that HepG-2 cells adhered onto culture plate, and the cell morphology keep long spindle, nucleus integrity and cells plumping after treated with mZnO/PLGA/GE. These cell morphologies were similar to the control, which indicated no toxicity of the mZnO/PLGA/GE under the conditions of this experiment. However, the HepG-2 cells treated with CPT/DOX@mZnO/PLGA/GE composite nanofibers acquired a round shaped morphology and a sharply decreased cell number for 24 h and 48 h **(Fig. 8)**. Furthermore, the red fluorescence of DOX and blue fluorescence of CPT in the cells were clearly observed for CPT/DOX@mZnO/PLGA/GE composite nanofibers (**Fig.**

8). The results suggest that both DOX and CPT released from the composite nanofibers were cytotoxic activity on HepG-2 cells. In addition, the HepG-2 cells morphologies treated with DOX/PLGA/GE and DOX@mZnO/PLGA/GE composite nanofibers were similar to that of CPT/DOX@mZnO/PLGA/GE composite nanofibers (**Fig. S4**). And these cell morphology results corroborate the MTT data, suggesting that the encapsulated anticancer within composite nanofibers displays non-compromised antitumor activity. The all results suggest the composite nanofiber encapsulated with DOX and CPT showed efficient and long-term antitumor efficacy, which might be used as local implantable scaffolds for potential postsurgical cancer treatment.

-----Fig. 8----

Conclusions

In this work, the PLGA/GE electrospun fibers encapsulated with DOX@mZnO were successfully fabricated, which enabled the delivery of two drugs with distinct rates. The addition of GE increased the hydrophilicity of PLGA/GE composite fibers. The introduction of DOX@mZnO significantly improved the mechanical properties of PLGA/GE fibers, furthermore the initial burst release of DOX was appreciably weakened and the release time was prolonged. The *in vitro* release results showed that CPT was released in a rapid rate due to the hydrophilic of GE in the PLGA/GE matrixes, while DOX showed a sustained and long term release behavior because of the hindrance of mZnO and PLGA/GE matrixes. The cell cytotoxicity test demonstrated that the composite nanofiber CPT/DOX@mZnO/PLGA/GE showed the strong cell growth inhibition. All the results suggested that the co-delivery system based on CPT/DOX@mZnO/PLGA/GE fibers was an excellent carrier for controllable delivery of both hydrophilic drug (DOX) and hydrophobic drug (CPT). And the composite fibers loaded with proper drugs might be a potential implantable scaffold in wound healing or implant in surgery for postsurgical cancer treatment.

Acknowledgements

Financial support for this work was provided by the National Natural Science Foundation of China (No.21164007 and 51203073). Jun Hu and Ming Li contributed equally to this work.

References

1. K. X. Qiu, C. L. He, W. Feng, W. Z. Wang, X. J. Zhou, Z. Q. Yin, L. Chen, H. S. Wang and X. M. Mo, *Journal of Materials Chemistry B*, 2013, 1, 4601-4611.
2. X. L. Xu, X. S. Chen, Z. F. Wang and X. B. Jing, *European Journal of Pharmaceutics and Biopharmaceutics*, 2009, 72, 18-25.
3. S. T. Yohe, V. L. Herrera, Y. L. Colson and M. W. Grinstaff, *Journal of Controlled Release*, 2012, 162, 92-101.
4. K. E. Uhrich, S. M. Cannizzaro, R. S. Langer and K. M. Shakesheff, *Chemical reviews*, 1999, 99, 3181-3198.
5. S. Chakraborty, I. Liao, A. Adler and K. W. Leong, *Advanced drug delivery reviews*, 2009, 61, 1043-1054.
6. Z. Sun, E. Zussman, A. L. Yarin, J. H. Wendorff and A. Greiner, *Advanced Materials*, 2003, 15, 1929-1932.
7. A. L. Yarin, E. Zussman, J. Wendorff and A. Greiner, *Journal of Materials Chemistry*, 2007, 17, 2585-2599.
8. X. L. Wang, H. W. Wang, M. X. Guo and Z. Huang, *Photodiagnosis and Photodynamic Therapy*, 2007, 4, 88-93.
9. B. T. Song, C. T. Wu and J. Chang, *Journal of Biomedical Materials Research Part B: Applied Biomaterials*, 2012, 100, 2178-2186.
10. F. Ahmed, R. I. Pakunlu, A. Brannan, F. Bates, T. Minko and D. E. Discher, *Journal of Controlled Release*, 2006, 116, 150-158.
11. L. Wei, C. H. Cai, J. P. Lin and T. Chen, *Biomaterials*, 2009, 30, 2606-2613.
12. Z. Y. Hou, X. J. Li, C. X. Li, Y. L. Dai, P. A. Ma, X. Zhang, X. J. Kang, Z. Y. Cheng and J. Lin, *Langmuir*, 2013, 29, 9473-9482.
13. H. L. Jiang, Y. Q. Hu, Y. Li, P. C. Zhao, K. J. Zhu and W. L. Chen, *Journal of Controlled Release*, 2005, 108, 237-243.
14. Y. Z. Zhang, X. Wang, Y. Feng, J. Li, C. T. Lim and S. Ramakrishna, *Biomacromolecules*, 2006, 7, 1049-1057.
15. J. Hu, J. C. Wei, W. Y. Liu and Y. W. Chen, *Journal of Biomaterials Science, Polymer Edition*, 2013, 24, 972-985.

16. H. X. Qi, P. Hu, J. Xu and A. J. Wang, *Biomacromolecules*, 2006, 7, 2327-2330.
17. X. L. Xu, L. X. Yang, X. Y. Xu, X. Wang, X. S. Chen, Q. Z. Liang, J. Zeng and X. B. Jing, *Journal of controlled release*, 2005, 108, 33-42.
18. R. L. Qi, R. Guo, M. W. Shen, X. Y. Cao, L. Q. Zhang, J. J. Xu, J. Y. Yu and X. Y. Shi, *Journal of Materials Chemistry*, 2010, 20, 10622-10629.
19. F. Y. Zheng, S. G. Wang, M. W. Shen, M. F. Zhu and X. Y. Shi, *Polymer Chemistry*, 2013, 4, 933-941.
20. B. T. Song, C. T. Wu and J. Chang, *Acta biomaterialia*, 2012, 8, 1901-1907.
21. A. El-Fiqi and H.-W. Kim, *RSC Advances*, 2014, 4, 4444-4452.
22. E. Jo, S. Lee, K. T. Kim, Y. S. Won, H. S. Kim, E. C. Cho and U. Jeong, *Advanced Materials*, 2009, 21, 968-972.
23. Y. Z. Wang, W. L. Qiao, B. C. Wang, Y. Q. Zhang, P. Y. Shao and T. Y. Yin, *Polymer journal*, 2011, 43, 478-483.
24. P. B. Zhang, Z. K. Hong, T. Yu, X. S. Chen and X. B. Jing, *Biomaterials*, 2009, 30, 58-70.
25. J. Y. Lee, C. A. Bashur, A. S. Goldstein and C. E. Schmidt, *Biomaterials*, 2009, 30, 4325-4335.
26. Z. X. Meng, Y. S. Wang, C. Ma, W. Zheng, L. Li and Y. F. Zheng, *Materials Science and Engineering: C*, 2010, 30, 1204-1210.
27. S. B. Lee, H. W. Jeon, Y. W. Lee, Y. M. Lee, K. W. Song, M. H. Park, Y. S. Nam and H. C. Ahn, *Biomaterials*, 2003, 24, 2503-2511.
28. M. S. Kim, I. Jun, Y. M. Shin, W. Jang, S. I. Kim and H. Shin, *Macromolecular Bioscience*, 2010, 10, 91-100.
29. K. Barick, S. Nigam and D. Bahadur, *Journal of Materials Chemistry*, 2010, 20, 6446-6452.
30. H. B. Bakrudeen, J. Tsibouklis and B. S. Reddy, *Journal of nanoparticle research*, 2013, 15, 1-13.
31. A. F. Wang, W. X. Qi, N. Wang, J. Y. Zhao, F. Muhammad, K. Cai, H. Ren, F. X. Sun, L. Chen and Y. J. Guo, *Microporous and Mesoporous Materials*, 2013, 180, 1-7.

32. S. Mitra, B. Subia, P. Patra, S. Chandra, N. Debnath, S. Das, R. Banerjee, S. C. Kundu, P. Pramanik and A. Goswami, *Journal of Materials Chemistry*, 2012, 22, 24145-24154.
33. K. C. Barick and D. Bahadur, *Journal of Nanoscience and Nanotechnology*, 2007, 7, 1935-1940.
34. S. K. Sahu, S. Maiti, T. K. Maiti, S. K. Ghosh and P. Pramanik, *Macromolecular Bioscience*, 2011, 11, 285-295.
35. K. C. Barick, M. Aslam, V. P. Dravid and D. Bahadur, *Journal of Physical Chemistry C*, 2008, 112, 15163-15170.
36. H. M. Nie, B. W. Soh, Y.-C. Fu and C.-H. Wang, *Biotechnology and Bioengineering*, 2008, 99, 223-234.
37. S. Y. Chew, T. C. Hufnagel, C. T. Lim and K. W. Leong, *Nanotechnology*, 2006, 17, 3880-3891.
38. D. Puppi, A. M. Piras, N. Detta, D. Dinucci and F. Chiellini, *Acta biomaterialia*, 2010, 6, 1258-1268.
39. A. Doustgani, E. Vasheghani-Farahani, M. Soleimani and S. Hashemi-Najafabadi, *Composites Part B-Engineering*, 2012, 43, 1830-1836.
40. M. Sun, X. Li, B. Ding, J. Yu and G. Sun, *Journal of Colloid and Interface Science*, 2010, 347, 147-152.
41. A. K. Jaiswal, H. Chhabra, S. S. Kadam, K. Londhe, V. P. Soni and J. R. Bellare, *Materials Science & Engineering C-Materials for Biological Applications*, 2013, 33, 2926-2936.
42. Z. X. Meng, W. Zheng, L. Li and Y. F. Zheng, *Materials Chemistry and Physics*, 2011, 125, 606-611.
43. Z. X. Meng, X. X. Xu, W. Zheng, H. M. Zhou, L. Li, Y. F. Zheng and X. Lou, *Colloids and Surfaces B-Biointerfaces*, 2011, 84, 97-102.

Table 1. Analysis of Water Contact Angles

Sample (fibers)	Contact angle/ deg±SD at 1s	Contact angle/ deg±SD at 30s	Contact angle/ deg±SD at 60s
PLGA	125±0.9	119.5±5.5	119±1.2
PLGA/GE	115±0.8	55±7.8	36±4.9
DOX/PLGA/GE	15.5±0.8	0	0
DOX@mZnO/PLGA/GE	36±0.5	0	0
CPT/DOX@mZnO/PLGA/GE	41±1.4	0	0

Table 2. Mechanical properties of nanofibers

Sample (fibers)	Tensile Strength/ MPa±SD	Elongation/ %±SD	Modulus/ MPa±SD
PLGA	2.5±0.2	109.2±18.8	154.7±12.5
PLGA/GE	1.9±0.3	50.5±0.7	47.3±12.1
DOX/PLGA/GE	2.7±0.1	47.5±3.5	79.7±3.7
DOX@mZnO/PLGA/GE	3.1±0.5	38.2±6.5	136.5±5.3

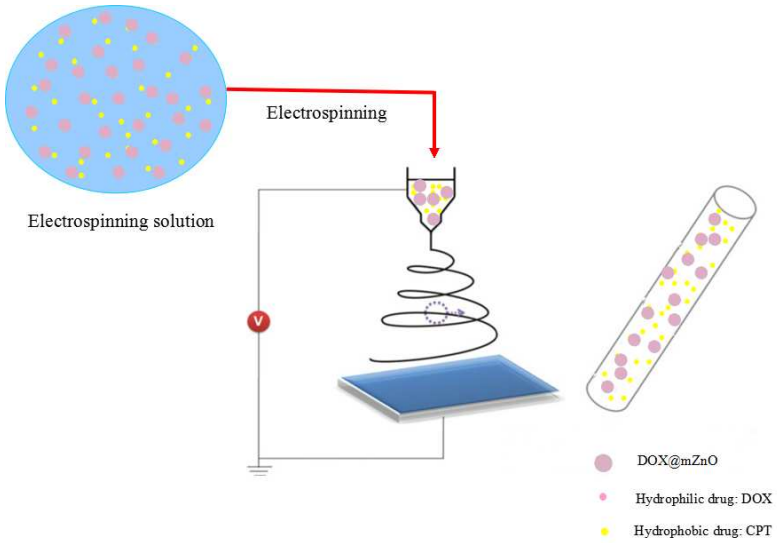

Fig. 1 Schematic illustration of the process of fabrication of dual drug-loaded electrospun composite fiber and the position of the two model drugs located in the fiber.

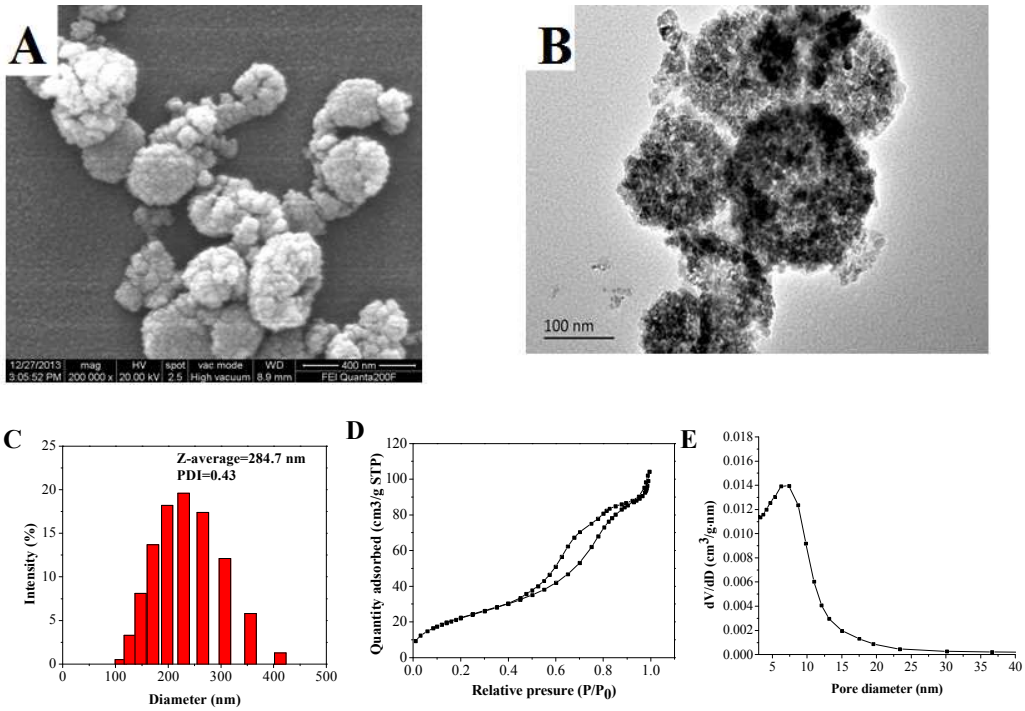

Fig. 2 The morphology, size distribution and structure of mZnO. (A) SEM image, (B) TEM image, (C) size distribution, (D) nitrogen adsorption-desorption isotherms and (E) the pore size distribution of mZnO.

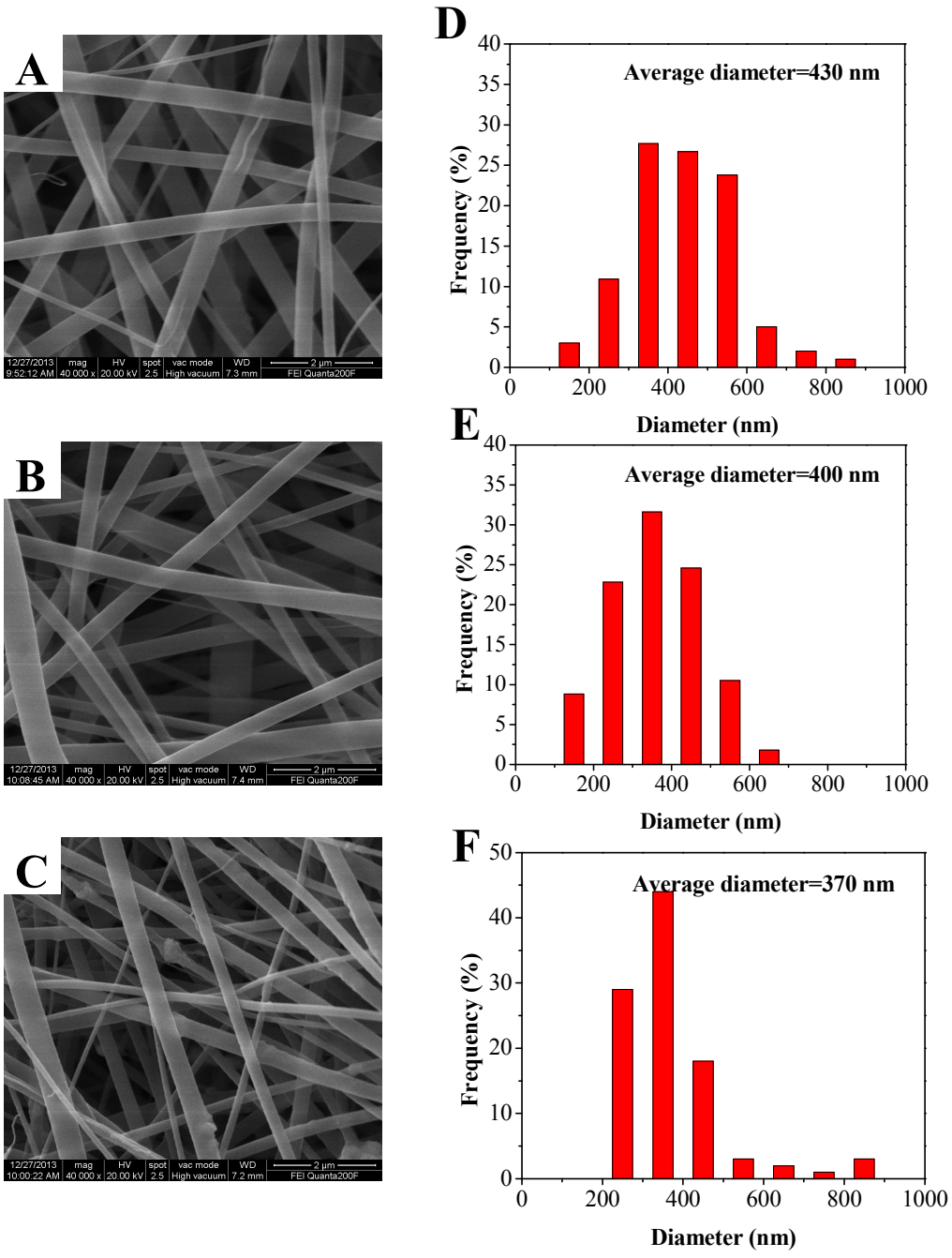

Fig. 3 SEM images of electrospun (A) PLGA/GE fibers, (B) DOX/PLGA/GE fibers and (C) DOX@mZnO/PLGA/GE fibers, and (D, E, F) the corresponding diameter distributions.

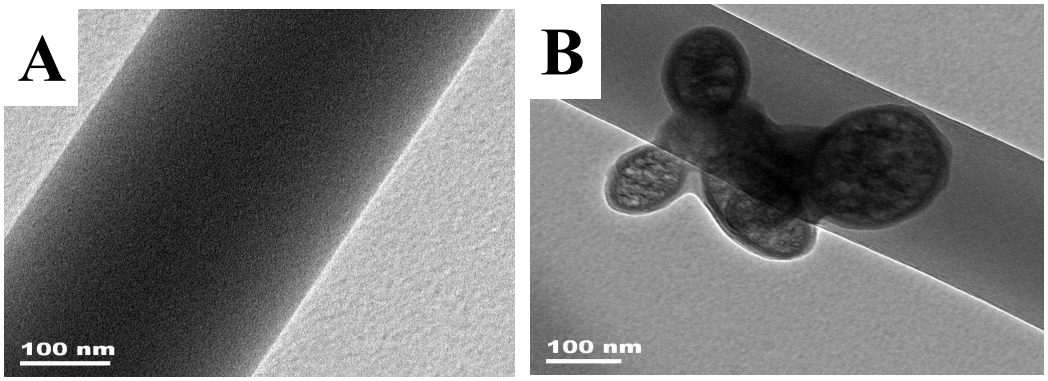

Fig. 4 TEM images of electrospun (A) PLGA/GE fibers and (B) DOX@mZnO/PLGA/GE fibers.

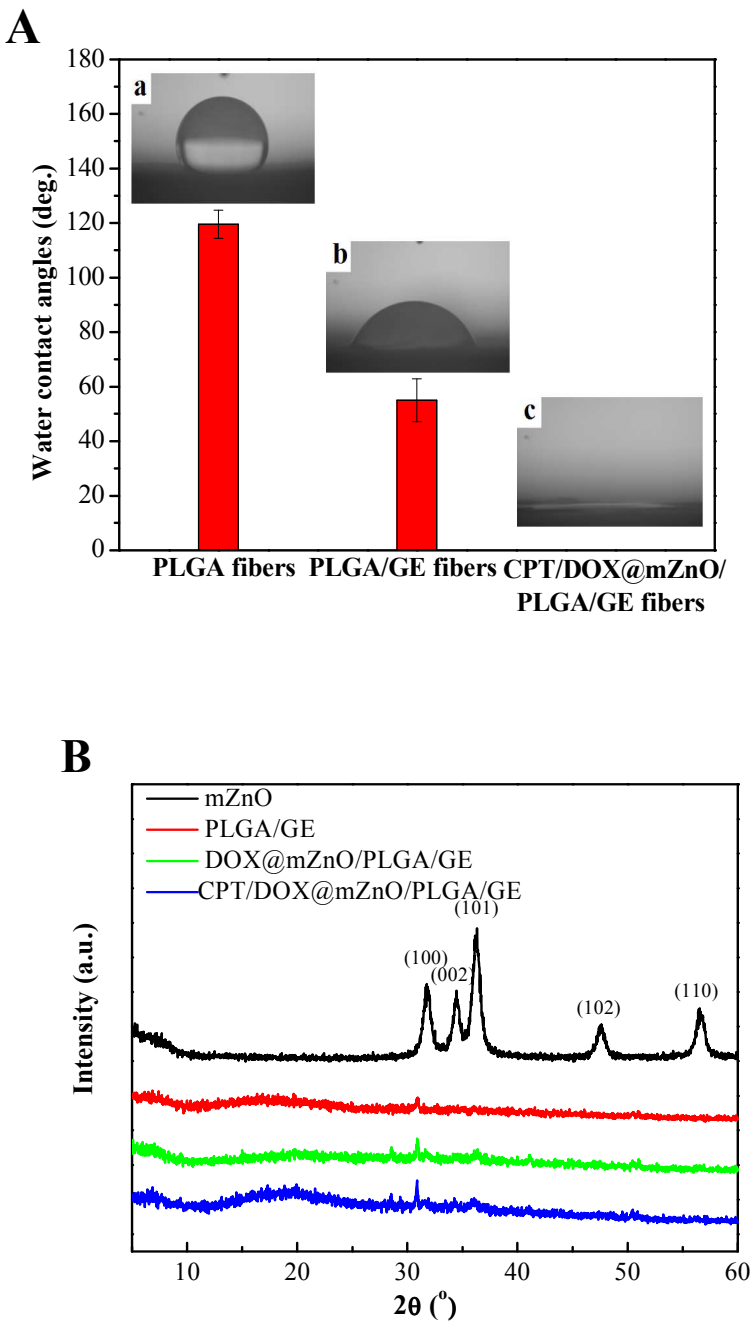

Fig. 5 Physico-chemical properties of the composite nanofibers: (A) The contact angle of (a) neat PLGA, (b) PLGA/GE and (c) CPT/DOX@mZnO/PLGA/GE fibers at 30 s; (B) The XRD patterns of mZnO, PLGA/GE, DOX@mZnO/PLGA/GE and CPT/DOX@mZnO/PLGA/GE.

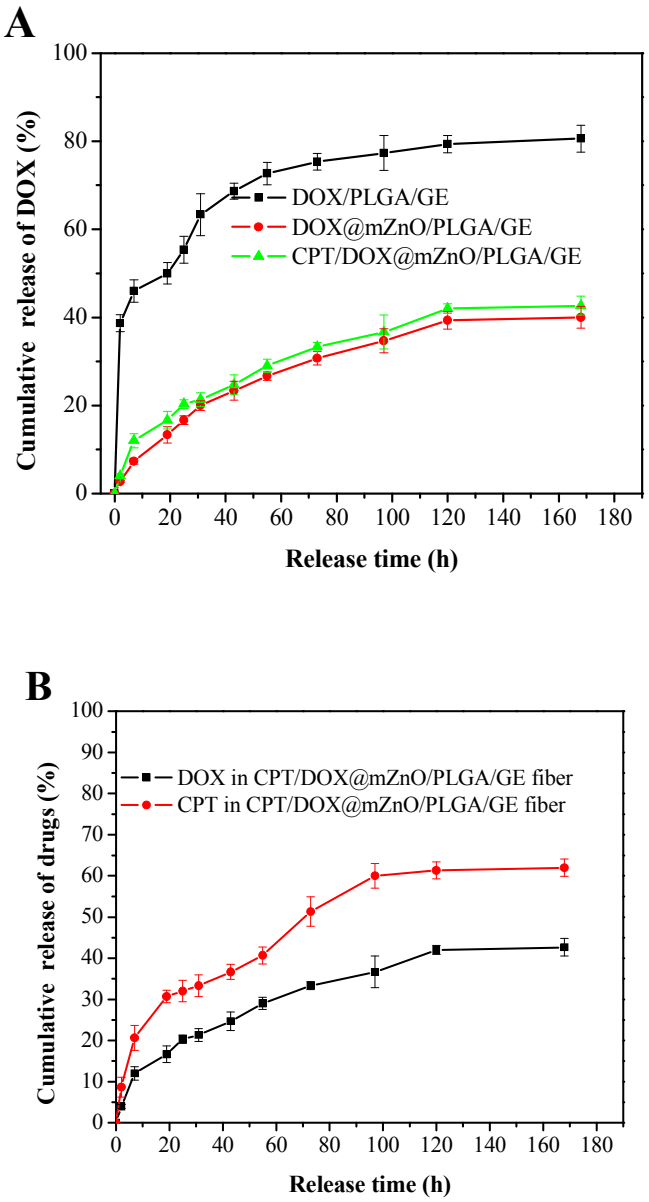

Fig. 6 (A) The cumulative DOX release from DOX/PLGA/GE, DOX@mZnO/PLGA/GE and CPT/DOX@mZnO/PLGA/GE composite nanofibers; (B) The cumulative DOX and CPT release from CPT/DOX@mZnO/PLGA/GE composite nanofibers in PBS (pH=7.4) at 37 °C.

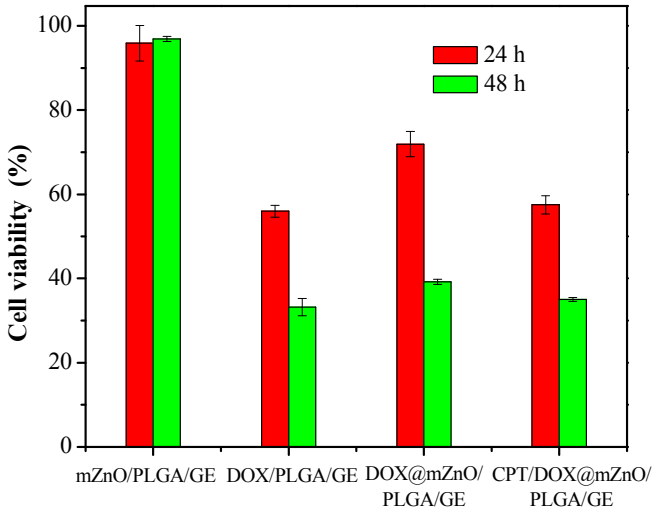

Fig.7 Cell viability of HepG-2 cells treated with different fibers for 24 h and 48 h.

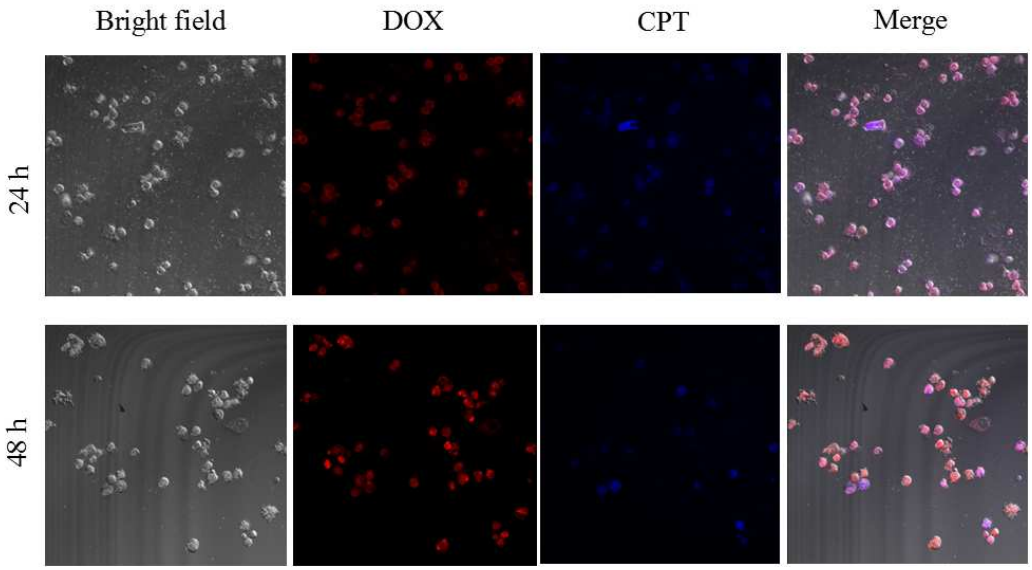

Fig. 8 CLSM images of HepG-2 cells treated with CPT/DOX@mZnO/PLGA/GE composite nanofibers for 24 h and 48 h. DOX concentration was 25 μg/mL. Red and blue fluorescence respectively represent the released DOX and CPT.

Highlights

Multiple Drugs-loaded Electrospun PLGA/gelatin Composite Nanofibers Encapsulated with Mesoporous ZnO Nanospheres for Potential Postsurgical Cancer Treatment

Jun Hu, Ming Li, Junchao Wei, Yong Chen, Yiwang Chen

The novel PLGA/GE fibers encapsulated with DOX@mZnO were successfully fabricated, which enabled the delivery of two drugs with distinct rates.

Graphical abstract